BL-6C/2019G635

Three-dimensional atomic configurations in a $ZnFe_2O_4$ single crystal by X-ray fluorescence holography

Shinya HOSOKAWA[1,*], Naohisa HAPPO[2], Koichi HAYASHI[3], and Tomohiro MATSUSHITA[4]

[1] Institute of Industrial Nanomaterials, Kumamoto University, Kumamoto 860-8555, Japan
[2] Graduate School of Information Sciences, Hiroshima City University, Hiroshima 731-3194, Japan
[3] Department of Physical Science and Engineering, Nagoya Institute of Technology, Nagoya 466-8555, Japan
[4] Division of Materials Science, Nara Institute of Science and Technology, Ikoma 630-0192, Japan

Three dimensional atomic structures of a zinc ferrite Franklinite $ZnFe_2O_4$ crystal was investigated by X-ray fluorescence holography with an atom-solved and element-selected functions. The obtained holograms were analyzed using a sparse modeling approach of a L_1-regression. From the present analysis, it was found that Zn and Fe atoms are perfectly located at tetrahedral A sites and octahedral B sites, respectively. This conclusion contradicts results of a neutron diffraction experiment, where site exchanges occurred between Zn and Fe atoms for fine particles by about 10–15% (T. Kamiyama et al., Solid State Commun. **81**, 563 (1992)).

1 Introduction

A zinc ferrite crystal of Franklinite $ZnFe_2O_4$ has a normal spinel structure [1]. This material achieved interests of only basic geology and crystallography sciences for a long time; however, it has recently attracted applicational interests as a cathode material for Li ion batteries since 2004 [2,3].

In the crystal, the O^{2-} anions form a cubic close packed structure, and the Zn^{2+} and Fe^{3+} cations preferentially occupy tetrahedral A and octahedral B sites, respectively. Note that the bond length in the A site is 0.1959 nm, which is slightly shorter than that in the B site of 0.2037 nm and would be affected by the cation radius with valencies, coordination numbers, and spin states.

There were several arguments on the occupations of cation atoms whether the Zn^{2+} and Fe^{3+} cations selectively enter the A and B sites, respectively, in the crystal or not. Kamiyama et al. [4] discussed the cation distributions in $ZnFe_2O_4$ fine particles by neutron powder diffraction. They reported a large size dependence of the Fe^{3+} occupancy at the tetrahedral A site of 10.8 (14.2) % with the crystal size of 0.960 (0.290) nm. The cation occupations in $ZnFe_2O_4$ were also studied by Jeyadevan et al. [5] with Fe and Zn *K* X-ray absorption fine structure (XAFS) measurements. The samples were manufactured by some different methods of usual sintering, coprecipitation (particle size of about 8 nm), and that annealed after the coprecipitated one. From the XAFS data as well as a remarkable increase of magnetization, it was concluded that Zn ions in the coprecipitated $ZnFe_2O_4$ are occupied both in A and B sites. On the other hand, it was not examined experimentally so far whether such an anomaly in cation distributions intrinsically exist even in large $ZnFe_2O_4$ crystal or not.

X-ray fluorescence holography (XFH) is a novel method for atom-resolved and element-selective structural characterizations and enables to draw three-dimensional (3D) atomic images around a specific element emitting fluorescent X-rays [6]. For reconstructing atomic images from measured holographic data, Barton's multi-wavelength method [7] based on the Fourier transform is typically used. However, atomic images reconstructed by this direct problem method frequently contain considerable artifacts, although a fundamental twin image problem is mostly solved. Since the intensities of the artifact reach about 30% of the maximum of the atomic images and unphysical negative signals remain by Barton's algorithm, however, a more sophisticated algorithm is necessary to clarify the present judgement for wrong distributions of Zn and Fe cation of about 10%.

Recently, we have utilized a new algorithm based on an inverse problem and representing sparse modeling approach [8] and applied it to some functional materials [9]. By using this algorithm, particularly, have succeeded in drawing weak image of less than 20% of the maximum value in a Mn-doped Bi_2Te_3 topological insulator [10]. In this paper, we report the results of Zn and Fe Kα XFH data of $ZnFe_2O_4$ single crystal analyzed by the new algorithm and discussed the cation distributions in this bulk spinel crystal.

2 Experiment and analysis

A single crystal of natural $ZnFe_2O_4$ was purchased at Crystal Base Co., Ltd. in Osaka, Japan, which was imported from SurfaceNet GmbH at Rheine,

Germany. The crystal had a flat (001) surface with a size of 10 × 10 mm^2 and a thickness of 0.5 mm. The crystallinity of the sample was confirmed by taking a Laue photograph.

Zn and Fe Kα XFH experiments on the $ZnFe_2O_4$ crystal were carried out at the beamline BL-6C of the Photon Factory located in the High Energy Accelerator Research Organization (PF-KEK) in Tsukuba, Japan. X-rays were focused onto the sample with a size of about 0.5 × 0.5 mm^2 by a sagittal cylindrical mirror. The sample was placed on a rotatable table for the incident angle θ and the azimuthal angle φ. The incident X-rays were focused with a size of 0.3 × 0.3 mm^2 on a (001) surface of the sample. The measurements were performed in inverse mode by changing $0° \le \theta \le 75°$ in steps of 1° and $0° \le \varphi \le 360°$ in steps of ~ 0.35° of the sample. The Zn (8.638 keV) and Fe (6.403 keV) *Kα* fluorescent X-rays were collected by an avalanche photodiode detector via a cylindrical graphite crystal energy-analyzer. The XFH signals were recorded at 13 different incident X-ray energies from 13.0 to 16.5 keV in steps of 0.25-0.50 keV for Zn *Kα* and at 15 different incident X-ray energies from 13.5 to 17.0 keV in steps of 0.25-0.50 keV for Fe *Kα*. Details of the experimental setup are given elsewhere [6].

The holographic oscillation data were obtained by normalizing the fluorescent X-ray intensities to the incident X-ray intensities measured with an ion chamber, and then, subtracting the backgrounds. Extensions of the holographic data to the 4π solid angles were carried out by the measured X-ray standing wave (XSW) lines in the holographic data with fourfold rotational symmetries around all the axes and three mirror symmetries in both the Zn and Fe *Kα* holograms.

To perfectly reconstruct atomic images, an infinite number of holograms are necessary for varying k from 0 to ∞. In Barton's algorithm, the Fourier integral is replaced by a sum of a limited number of holograms with different k values, which is the main reason for the appearance of artifacts in the reconstructed atomic images. To solve this problem, Matsushita developed a new algorithm, SPEA- L1 [8], based on an inverse problem and a sparse modeling. The details of this algorithm and excellent improvements of the atomic images by the L_1-regularized linear regression were clearly given in our research papers [10-13] and review papers [9, 14].

3 Results and Discussion

Figure 1 shows atomic images on the (001) plane around the Zn (upper) and Fe (lower) atoms. Ideal neighboring cation positions are indicated by large and small circles when the central atoms at the centers of the figures are located at the A and B sites, respectively. As seen in the figures, most of the neighboring atomic images are located at the ideal cation positions although small artifacts are mainly seen near the central atoms. A large difference is observed between the atomic images around the Zn and Fe atoms, i.e., atomic images are not seen at the B site around the Zn atom while distinct images are seen there around the Fe atom.

To quantitatively observe the cation occupancies, image intensities are exhibited in Fig. 2 along the dashed lines in Fig. 1 around the (a) Zn and (b) Fe atoms. For clarity, the curve around Zn is displaced by 0.6. As seen in Fig. 2(a), no atomic images are detected at the B site around the Zn atom. On the other hand, as seen in Fig. 2(b), distinct atomic images are observed at the B site around the Fe atom.

4 Conclusion

From the present analysis for the Zn and Fe *Kα* XFH, it was concluded that Zn and Fe atoms are perfectly located at tetrahedral A sites and octahedral B sites, respectively, in the $ZnFe_2O_4$ bulk crystal. This conclusion contradicts results of a neutron diffraction experiment, where site exchanges occurred between Zn and Fe atoms for fine particles by about 10–15% [4].

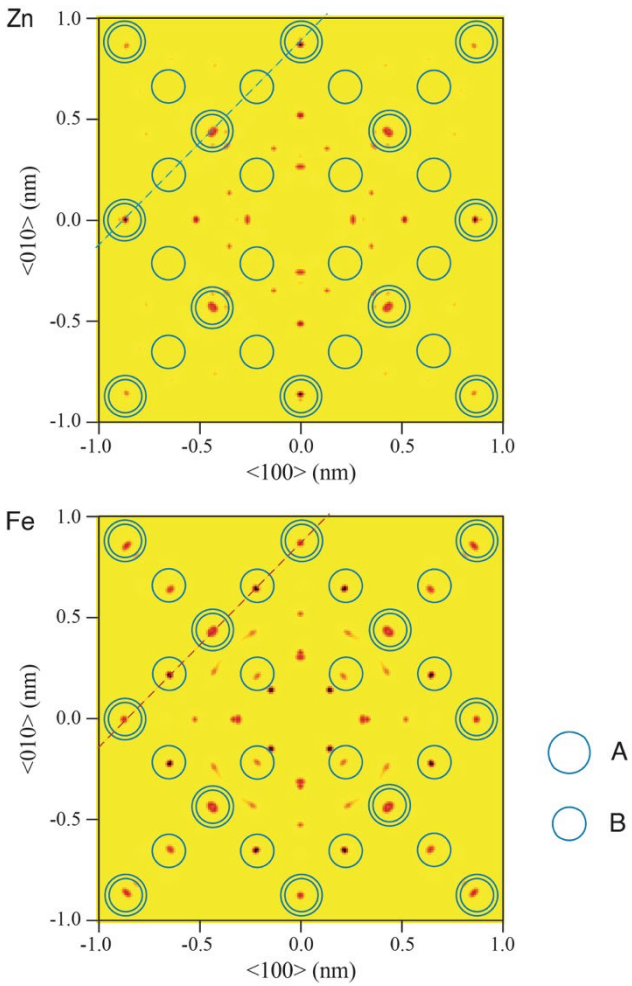

Fig. 1: Atomic images on the (001) plane around the Zn (upper) and Fe (lower) atoms.

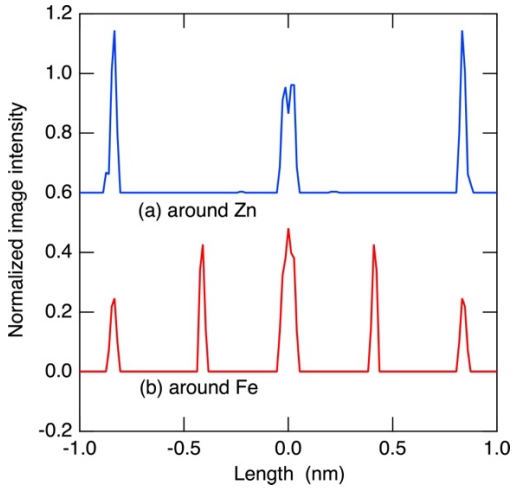

Fig. 2: Atomic distributions along the dashed lines in Fig. 1 around (a) Zn and (b) Fe atoms. For clarity, the curve around Zn is displaced by 0.6.

* shhosokawa@kumamoto-u.ac.jp

Acknowledgement

XFH measurements were carried out at BL6C in the PF-KEK (No. 2019G635). Financial supports by JSPS Grant-in-Aid for Transformative Research Areas (A) 'Hyper-Ordered Structures Science' are acknowledged (Nos. 21H05569 and 23H04117 for SH, No. 20H05881 for KH, and 20H05884 for TM). SH is also supported by JSPS Grant-in- Aid for Scientific Research (C) (No. 22K12662) and the Japan Science and Technology Agency (JST) CREST (No. JPMJCR1861).

References

[1] J. C. Waerenborgh *et al.*, *J. Solid State Chem.* **111**, 300 (1994).
[2] Y. N. Li *et al., J. Electrochem. Soc.* **151**, A1077 (2004).
[3] M. Bini *et al., Appl. Sci.* **11**, 11713 (2021).
[4] T. Kamiyama et al., *Solid State Commum*. **81**, 563 (1992).
[5] B. Jeyadevan et al., *J. Appl. Phys.* **76**, 6325 (1994).
[6] K. Hayashi et al., *J. Phys.: Condens. Matter* **24**, 093201 (2012).
[7] J. J. Barton, *Phys. Rev. Lett.* **67**, 3106 (1991).
[8] T. Matsushita, *e-J. Surf. Sci. Nanotechnol*. **14**, 158 (2016).
[9] S. Hosokawa et al., *Phys. Status Solidi B* **255**, 1800089 (2018).
[10] S. Hosokawa et al., *Phys. Rev. B* **96**, 214207 (2017).
[11] S. Hosokawa et al., *J. Phys. Soc. Jpn*. **89**, 034603 (2020).
[12] S. Hosokawa et al., *e-J. Surf. Sci. Nanotechnol*. **20**, 36 (2022).
[13] N. Happo et al., e-J. Surf. Sci. Nanotechnol. **20**, 51 (2022).
[14] T. Matsushita et al., *J. Phys. Soc. Jpn*. **87**, 061002 (2018).